Pulmonary Research Day

Thursday, March 9, 2017

Abstract Book

Division of Pulmonary and Critical Care Medicine

Washington University in St. Louis

SCHOOL OF MEDICINE

Basic Category

MuscleDB: An open source cloud based platform for visualizing RNA-seq data

Scott A. Lewis[1], Erin E. Terry[1], Jiajia Li[1], Laura D. Hughes[1], Xiping Zhang[2], Jon England[3], Elizabeth Schroder[3], Ming Gong[3], Francisco Andrade[3], Karyn A. Esser[2], and Michael E. Hughes[1,4]

[1]Washington University School of Medicine, St. Louis, Missouri, USA. [2]Department of Physiology and Functional Genomics, University of Florida, Gainesville, Florida, USA. [3]College of Medicine, University of Kentucky, Lexington, Kentucky, USA. [4]Michael.hughes@wustl.edu

In order to address the challenges involved in managing a broad range of RNA sequencing data we have developed an online, open source RNA-seq database – MuscleDB – which systematically profiles transcriptional diversity between different skeletal muscle tissues. Thousands of genes are differentially expressed between different skeletal muscles, underscoring the remarkable specialization of these tissues and providing an opportunity to understand the genetic pathways underlying muscle specialization and susceptibility to different pathologies.

Achilles is a circadian clock-controlled gene that regulates immune function in _Drosophila_

Jiajia Li[a,b], Erin E. Terry[a], Edith Fejer[c], Diana Gamba[b], Natalie Hartmann[b], Joseph Logsdon[b], Daniel Michalski[b], Lisa E. Rois[b], Maria J. Scuderi[c], Michael Kunst[d], Michael E. Hughes[a]
[a]Division of Pulmonary and Critical Care, Department of Internal Medicine, Washington University in St. Louis, St. Louis, MO. [b]Department of Biology, University of Missouri – St. Louis, St. Louis, MO. [c]Department of Chemistry, University of Missouri – St. Louis, St. Louis, MO. [d]Department of Genes – Circuits – Behavior, Max Planck Institute of Neurobiology, Martinsried, 82152, Germany

The circadian clock is a transcriptional/translational feedback loop that drives the rhythmic expression of downstream mRNAs. Termed "clock-controlled genes," these molecular outputs of the circadian clock orchestrate cellular, metabolic, and behavioral rhythms. As part of our on-going work to characterize key upstream regulators of circadian mRNA expression, we have identified a novel clock-controlled gene in *Drosophila melanogaster*, *Achilles* (*Achl*), which is rhythmic at the mRNA level in the brain and which represses expression of antimicrobial peptides in the immune system. Achilles knock-down in neurons dramatically elevates expression of crucial immune response genes, including *IM1* (*Immune induced molecule 1*), *Mtk* (*Metchnikowin*), and *Drs* (*Drosomysin*). As a result, flies with knocked-down *Achilles* expression are resistant to bacterial challenges. Meanwhile, no significant change in core clock gene expression and locomotor activity is observed, suggesting that *Achilles* influences rhythmic mRNA outputs rather than directly regulating the core timekeeping mechanism. Notably, *Achilles* knock-down in the absence of immune challenge significantly diminishes the fly's overall lifespan, indicating a behavioral or metabolic cost of constitutively activating this pathway. Together, our data demonstrate that (1) *Achilles* is a novel clock-controlled gene that (2) regulates the immune system, and (3) participates in signaling from neurons to immunological tissues.

Disease mutations in TREM2 reveal a functional surface and two distinct loss-of-function mechanisms

Daniel L Kober[1,2,5], Jennifer M. Alexander-Brett[2,5], Michael J. Holtzman[2,3,5], and Tom J. Brett[2,3,4,5]

[1]Molecular Biology and Microbial Pathogenesis; [2]Department of Internal Medicine; [3]Cell Biology & Physiology; [4]Biochemistry & Molecular Biophysics; [5]Drug Discovery Program in Pulmonary and Critical Care Medicine Washington University School of Medicine, St. Louis, MO

Introduction: Triggering receptor expressed on myeloid cells-2 (TREM2) is an innate immune receptor that regulates myeloid cell activation in a variety of pathologies including inflammatory pulmonary disease such as COPD. In an animal model of COPD, TREM2 is required for macrophage survival and proliferation. Despite its importance, the endogenous ligands for TREM2 are unknown and there is a deficiency of information regarding its structure and mechanism. Distinct coding variants in the TREM2 Ig domain have been linked to the severe dementia known as Nasu-Hakola disease (NHD) or Alzheimer's disease (AD). It is unknown how different mutations to the same protein domain result in different pathologies. We hypothesized understanding how these variants alter TREM2 structure and function would shed light on this key protein.

Methods: We performed structural, biophysical, and functional studies to elucidate the molecular mechanisms underlying TREM2-associated pathologies. We developed a novel mammalian-cell expression system for TREM2, crystallized the Ig domain, and determined its structure at 3.1 Å.

Results: We used our hTREM2 crystal structure to generate hypotheses regarding the role of disease variants and TREM2 function. Analysis of the structure revealed the NHD residues are buried while the AD residues are solvent exposed, suggesting the NHD mutations destabilize the protein while AD mutations impact ligand binding. Extensive biochemical and biophysical experiments demonstrate the NHD mutations disrupt protein stability and reduce surface expression of folded protein while the AD mutations are not grossly altered in structure or stability. Next, we addressed the nature of the TREM2 ligand and asked whether AD mutants disrupt binding. We found TREM2 binds a specific protein ligand on mammalian cells through a glycosaminoglycan-dependent mechanism. AD mutations, including R47H, disrupt binding to this ligand while a T96K variant (which has unclear disease risk) increases binding. These variants epitope map a functional ligand-binding surface on the TREM2 protein that is unique within the overall TREM family. Our ongoing work is addressing the full identity of the TREM2 ligand complex.

Conclusions: Our findings reveal two distinct loss-of-function mechanisms for disease-linked mutations. NHD mutations cause misfolding while AD mutations do not grossly impact structure or stability. TREM2 binds a protein-dependent ligand on mammalian cells and AD-linked mutations disrupt this interaction. These novel findings will inform patient-specific molecular therapies targeting TREM2 for the treatment of inflammatory pulmonary and neurodegenerative disorders.

CLCA1-mediated activation of TMEM16A to restore anion currents in CF airway cells

Kayla Berry, Monica Sala-Rabanal, Zeynep Yurtsever, Colin G. Nichols, and Tom J. Brett
Cell Biology and Physiology, CIMED, and Pulmonary and Critical Care Medicine, Washington University School of Medicine, St. Louis, MO

CLCA1 (calcium-activated chloride channel regulator 1) is a secreted, self-cleaving protein that activates calcium activated chloride currents. We recently demonstrated that the N-terminal fragment of CLCA1 directly engages the calcium activated chloride channel TMEM16A, which stabilizes its surface expression and increases channel density, which thereby increases anion currents, Since CLCA1 directly engages TMEM16A, we hypothesized that this molecular recognition could be utilized to specifically activate anion currents in airway epithelia through TMEM16A to compensate for the dysfunctional CFTR channel in cystic fibrosis. This strategy has the potential to restore chloride currents in CF patients regardless of genotype. First, we demonstrated that TMEM16A is specifically activated by CLCA1 and not other CLCA family members (CLCA2 and CLCA4). Next, we examined the localization of TMEM16A in CF lungs. We stained CF lung tissue sections (genotype homozygous deltaF508) with anti-TMEM16A antibody and found TMEM16A expression in apical airway epithelium as well as in submucosal glands. Finally, to begin to test whether CLCA1 may activate TMEM16A currents in CF, we cultured primary CF airway cells (genotypes delF508/2789+5G>A, delF508/2184insA and delF508/delF508), exogenously applied CLCA1 for 24 hours, and performed whole-cell patch clamp experiments. CLCA1 was found to increase chloride currents above control. These currents were blocked by the TMEM16A inhibitor $T16A_{inh}$-A01. These preliminary results indicate that CLCA1 can specifically increase chloride currents through TMEM16A in CF airway epithelium. Further studies will be required to investigate whether activation of TMEM16A currents via CLCA1 can increase chloride currents in CF airway epithelium of other genotypes and whether it may restore healthy mucous properties and to determine the structural basis for CLCA1/TMEM16A interaction.

Cilia motion analysis in human airway epithelial cells: in vitro vs ex vivo

A. Oltean[1,2], A. J. Schaffer[1], P. V. Bayly[2], S. L. Brody[1]

[1]Division of Pulmonary and Critical Care Medicine, Washington University School of Medicine, St. Louis, MO, US. [2]Department of Mechanical Engineering and Material Science, Washington University, St. Louis, MO, US

Introduction: Primary ciliary dyskinesia (PCD) is a disease caused by genetic mutations in proteins required for motile cilia structure and function. Abnormal or incomplete cilia motion in PCD can cause situs inversus, infertility, and chronic respiratory infections. Diagnosing this genetic disorder involves technical expertise to analyze multiple tests such as nasal nitric oxide, electron microscopy to assess cilia structure, genotyping, and high speed video microscopy of cilia motion. While some diseased cells have obvious defects in cilia motion such as paralyzed cilia, other changes in cilia function may be subtle or too difficult to ascertain by eye with subjective descriptors.

Methods: To properly diagnosis abnormal cilia function, we sought to first define the characteristics of a healthy cilia waveform and the variation within samples or across cells obtained from non-diseased donors. We examined tracheobronchial epithelial cells from ex vivo samples and primary-culture cells over the course of ciliogenesis in vitro. We recorded cilia motion on the side view of cells scraped from an airway mounted on a microscope slide or the top view of cells grown on a membrane at an air-liquid interface. Using high speed video capture with a high magnification objective, we analyzed cilia motion and quantified cilia parameters such as length and beat frequency.

Results: Our data suggest large variation in waveform shape that depends on variables such as cilia length, cilia beat frequency, stroke width, and stage of differentiation. During in vitro ciliogenesis, we found that parameters of cilia function and waveform change and are different from the cilia motion observed in ex vivo samples.

Conclusion: By comparing in vitro and ex vivo samples, we have observed large variation in many parameters of cilia motion. We hope to determine the most useful, objective parameters to describe cilia motion, with the ultimate goal of characterizing cells as healthy or diseased using high speed video microscopy.

Human Airway Epithelial Cells Have Multiple Sources And Stores Of The Intracellular Complement Protein C3.

H.S. Kulkarni[1], M.L. Elvington[2], M.K. Liszewski[2], S.L. Brody[3], J.P. Atkinson[2]
Divisions of [1]*Pulmonary and Critical Care Medicine and* [2]*Rheumatology, Department of Medicine, Washington University in Saint Louis*

Introduction: The complement system is a fundamental mechanism for host defense, including at the air-liquid interface, where it can deal with environmental stress. Its central component C3 is an abundant blood protein that can be cleaved to C3a, an anaphylatoxin, and C3b, an opsonin. We recently found that airway epithelial cells (AECs) contain abundant intracellular stores of C3. Certain cell types load C3 as C3(H2O) [form of C3 lacking an intact thioester bond] from the blood in a rapid, saturable manner. However, the source and stores of C3 in AECs is not defined.

Methods: Both the BEAS-2B cell line and primary culture human tracheobronchial epithelial cells (hTEC) were employed. C3 mRNA was determined using RT-PCR, and protein by immunoblot analysis. C3 uptake was determined using media containing normal human serum, and purified C3. The precursor form of C3 (proC3) was distinguished from native C3 (nC3) by using dithiothreitol (DTT) to reduce C3 into its alpha and beta chains. Subcellular protein fractions were sequentially obtained from the cytoplasm, membranes, nucleus, chromatin and cytoskeleton.

Results: BEAS2B and hTEC cultured in serum-free media (C3-free) had a 190kDa protein corresponding to purified C3 that was not present in cell lines such as Farage (B cell), Jurkat (T cell) and ARPE (retina). On treatment of BEAS-2B and hTEC cell lysates with dithiothreitol (DTT), only a fraction of the 190kDa protein reduced to the C3 alpha and beta chains as determined by protein standards, while the rest remained at 190kDa, consistent with the precursor form (proC3). This indicates at least two distinct forms of intracellular C3 – nC3 and proC3. AEC culture in normal serum resulted in C3(H2O) uptake within 15 minutes and on DTT treatment, C3(H2O) was entirely reduced to the alpha and beta chains. Upon uptake, C3(H2O) was detected in all the subcellular fractions, indicating rapid redistribution within the compartments. The AEC supernatant contained both C3 and the anaphylatoxin, C3a by 48 hours, suggesting that AECs constitutively and continuously synthesized C3. Addition of protease inhibitors abrogated C3 cleavage, suggesting that AECs constitutively secrete proteases that cleave locally formed C3.

Conclusions: Airway epithelial cells contain two sources for intracellular C3 – via biosynthesis and uptake. Their intracellular stores contain distinct forms – both C3 and C3(H2O). Upon AEC activation, these stores are released and become local sources of C3, from which proteases produce C3a. These represent novel pathways for complement-mediated local defense for continued surveillance in the airway.

IL-13 Regulates MAPK13 Expression and Activation to Drive Excess Airway Mucus Production

Benjamin J. Gerovac, Yael G. Alevy, Jennifer Yantis, Jian Xu, Rowena Grainger, Steven L. Brody and Michael J. Holtzman
Pulmonary and Critical Care Medicine, Washington University of Medicine, St. Louis, Missouri.

Abstract: Mucin hypersecretion and mucous cell metaplasia are characteristics of respiratory diseases such as asthma and chronic obstructive pulmonary disease (COPD). Previous literature demonstrated that the cytokine interleukin-13 (IL-13) stimulates both mucous cell metaplasia and mucus secretion. In addition, data from primary-culture human tracheal epithelial cells (hTECs) showed that IL-13-dependent mucin expression requires mitogen-activated protein kinase 13 (MAPK13) phosphorylation as pharmacological inhibition of MAPK13 activity attenuates mucus production. Given that MAPK13 is required for IL-13 driven mucin expression, we aimed to determine if IL-13 might regulate MAPK13 expression. We found that IL-13 increases the levels of phosphorylated MAPK13 and total MAPK13 in hTEC cultures. The results unexpectedly suggest that IL-13 regulates the level of MAPK13 expression and activation to drive increases in airway mucus production and consequent obstructive airway disease.

Influenza A Virus Causes Chronic Inflammatory Airway Disease Linked Partially to IL-13 Expression

Shamus P. Keeler, M.E. Hinojosa, K. Wu, R.M. Tidwell, J.J. Atkinson, E. Agapov, and M.J. Holtzman
Drug Discovery Program, Pulmonary and Critical Care Medicine, Washington University School of Medicine, St. Louis, MO 63110

Introduction: Clinical and experimental observations suggest that the development of chronic lower respiratory disease is linked to respiratory viral infection and perhaps to the severity of infection. However, there is no experimental model that establishes the long-term aspect of this relationship using a potent human pathogen. Accordingly, we used influenza A virus (IAV) to develop a mouse model for severe respiratory viral infection that leads to chronic lung disease after clearance of infection, and we determined the immune basis for this type of disesse.

Methods: Inbred C57/BL/6J mice (wild-type and IL-13-deficient strains) were infected intranasally at 6 weeks of age with IAV (A/WS/33 strain) using a range of inoculum sizes. Animals were then studied at 1-12 days after infection to assess acute infectious illness and at 21-182 days after infection to assess chronic lung disease using immunohistochemistry as well as host and viral gene expression.

Results: Infection with IAV triggers chronic lung disease that was dependent on viral inoculum and in turn the severity of infection during the acute illness and was manifested by long-term airway inflammation, mucus production, and hyperreactivity in wild-type mice. Mucus production was localized to focal areas of inflammation within the lung, and these inflammatory foci and airway hyperreactivity persisted for at least 6 months after viral inoculation. Partial inhibition of post-viral airway mucus production and hyperreactivity was found in IL-13-deficient mice compared to wild-type control mice.

Conclusions: The results establish the capacity of a respiratory virus that causes acute illness in humans to also trigger chronic lower respiratory disease that is linked to acute viral level and in part to a chronic type 2-like immune response that is manifest by IL-13 production. The findings appear relevant to clinical observations that link severe influenza infections to exacerbations in humans with chronic lower respiratory diseases such as asthma and COPD and to observations that at least some of this pathology occurs independent of IL-13 expression.

Research Funding Source: NIH (NHLBI and NIAID).

Neuronal IL-4Rα and JAK1 signaling mediate chronic itch

Landon K. Oetjen[1], Madison R. Mack[1], Timothy M. Whelan[1], Changxiong J. Guo[2], Lihua Yang[3], Samantha L. Hamilton[3], Peter L. Wang[4], Haixia Niu[1], Jing Feng[2], Amy Z. Xu[1], Shivani V. Tripathi[1], Jialie Luo[2], Jonathan R. Brestoff[4], András Schaffer[1,4], Chyi-Song Hsieh[4,5], Robert W. Gereau, IV[2], Mark J. Miller[3], Hongzhen Hu[2], Steve Davidson[6], Qin Liu[2], and Brian S. Kim[1,2,4]

[1] Division of Dermatology, Department of Medicine, Washington University School of Medicine, St. Louis, MO 63110 USA.[2] Department of Anesthesiology, Washington University School of Medicine, St. Louis, MO 63110 USA.[3] Division of Infectious Diseases, Department of Medicine, Washington University School of Medicine, St. Louis, MO 63110 USA.[4] Department of Pathology and Immunology, Washington University School of Medicine, St. Louis, MO 63110 USA.[5] Division of Rheumatology, Department of Medicine, Washington University School of Medicine, St. Louis, MO 63110 USA. [6] Department of Anesthesiology, University of Cincinnati College of Medicine, Cincinnati, OH 45267 USA.

Introduction: Chronic pruritus, defined as symptoms of itch lasting longer than six weeks, affects up to 15% of the population and has a profoundly negative impact on quality of life. It is a central feature of many primary inflammatory skin disorders such as atopic dermatitis (AD), a disease driven by the type 2 cytokines IL-4 and IL-13. Further, chronic itch can commonly present in the absence of any known disease process, and, in this setting, has been described as chronic idiopathic pruritus (CIP). Despite the high incidence of chronic itch and its burden on quality of life, the cellular and molecular processes which underlie itch in human disease remain poorly understood. As a result, effective treatments for chronic itch are limited, and there are currently no FDA-approved medications specifically indicated for chronic pruritus.

Methods: In this study, we hypothesized that type 2 cytokines and their downstream signaling components directly promote chronic itch. We employed a combination of pharmacologic and sensory neuron-specific genetic approaches to investigate this possibility in a well-established mouse model of AD associated with robust itch. In proof-of-concept translational studies, we enrolled a small cohort of CIP patients (N=5) in a preliminary clinical trial using the JAK inhibitor tofacitinib.

Results: We found that sensory neurons are directly activated by IL-4 and IL-13 along previously defined itch-sensory pathways, supporting the hypothesis that neuronal type 2 cytokine signaling mediates chronic itch. Indeed, employing neuron-specific deletion of IL-4Rα, the shared receptor subunit for IL-4 and IL-13, we found that neuronal expression of IL-4Rα is critically required for the development of chronic itch. Based on IL-4Rα signaling biology, we thus hypothesized that dysregulated intracellular JAK signaling may be a conserved mechanism by which chronic itch is mediated. Strikingly, both pharmacologic JAK inhibition and sensory neuron-specific genetic deletion of JAK1 demonstrated abatement of chronic itch. Although JAK inhibitors are known as anti-inflammatory agents, whether they exhibit additional neuromodulatory properties is not known. In support of this possibility, we observed dramatic improvement of itch symptoms in a small cohort of CIP patients treated off-label with the JAK inhibitor tofacitinib after failing other anti-inflammatory therapies.

Conclusions: These results establish new molecular pathways by which both type 2 cytokine and JAK signaling in sensory neurons promote itch and provide strong rationale for targeting these pathways in chronic itch disorders.

CD2AP Regulates the T cell Response to Chronic Viral Infection

Saravanan Raju, Andrey S. Shaw, Takeshi Egawa
Department of Pathology and Immunology

CD2-Associated Protein (CD2AP) is a scaffolding molecule originally identified as a CD2 interacting partner, and now known to be essential for proper function of the glomerular filtration barrier. Previous work has suggested CD2AP plays a role in attenuation of antigen-induced signaling in T cells in vitro. However the *in vivo* function of CD2AP is unclear. To define the function of CD2AP, we generated T cell-specific CD2AP conditional knockout mice and examined T cell responses to pathogen infection. Although we found no defects in the T cell response to acute LCMV infection, control of chronic LCMV infection was enhanced in CD2AP conditional knockout mice. This enhanced control of infection was associated with increased T Follicular Helper response and increased number of germinal center B cells. CD2AP deficient T cells sustained their surface TCR expression following antigen stimulation specifically under TH1 conditions, but not TH2 conditions, and thus seemed to receive prolonged antigen receptor stimulation during viral infection, resulting in enhanced T Follicular Helper responses. We are currently investigating the molecular mechanism by which CD2AP functions in T cells.

Mitochondria release by lung transplantation promotes primary graft dysfunction

Davide Scozzi[1,4], Xue Lin[1], Ibrahim Mohsen[1], Derek E. Byers[3], Ramsey Hachem[3], Alexander S. Krupnick[1,2], Daniel Kreisel[1,2] and Andrew E. Gelman[1,2,&4]
Departments of [1]Surgery, [2]Pathology & Immunology, and [3]Medicine, Medicine Washington University School of Medicine, St. Louis, MO
[4]Department of Clinical and Molecular Medicine, Sapienza University of Rome, Italy

Introduction: Primary Graft Dysfunction (PGD), a common form of lung transplant-induced acute lung injury, is associated with high morbidity and mortality. The release of mitochondria by injured tissues has been shown to promote sterile inflammation through the activation of the Formylated Peptide Receptor 1 (FPR1). We hypothesized that the early release of mitochondria may exacerbate PGD by controlling the immune response to the graft.

Methods: BAL fluids obtained from human and mouse lung transplant recipients were analyzed for cell-free mitochondria accumulation using flow cytometry and transmission electron microscopy. To investigate the contribution of the mitochondria-FPR1 axis to the early graft injury we use an orthotopic mouse lung transplant model of PGD. Lung transplantations were performed where either the donor, the recipient or both were deficient for FPR1. Graft injury was assessed by H&E histopathology, wet to dry ratio and BAL fluid protein content. Intravital 2-photon microscopy and flow cytometry were used to analyze neutrophil activation, recruitment and intragraft distribution. In a study of 62 human lung transplant recipients, circulating plasma levels of mitochondria DNA (mtDNA) were measured early after transplant by quantitative PCR to investigate a possible association with PGD.

Results: In human and mouse lung transplant recipients we detected the release of intact donor-derived mitochondria into the injured airways. FPR1 promoted neutrophil scavenging of graft-derived mitochondria leading to enhanced ROS generation. Regardless to donor expression, FPR1 from the recipient was sufficient to worsen early graft injury compared to control mice. Surprisingly, FPR1 did not control overall neutrophil recruitment to the lung grafts but selectively augmented airway neutrophilia and inhibited neutrophil egress from the damaged airways. FPR1 also reduces neutrophil intragraft mobility increasing the stability of extravascular neutrophil clusters. In human lung transplant recipients circulating mtDNA plasma levels rose following transplantation and were highest in patients with persistent and severe PGD.

Conclusion: Our results suggest that mitochondria release contributes to PGD through altering FPR1 dependent neutrophil intragraft trafficking. Levels of circulating mtDNA may show promise as a biomarker to assess the development risk for severe PGD.

Splenic Monocytes Promote Neutrophil Extravasation into Lung Grafts via a IL1b-Dependent Pathway

H.-M. Hsiao, S. Tanaka, T. Takahashi, W. Li, D. Scozzi, Y. Liu, R. Higashikubo, A.S. Krupnick, A.E. Gelman, D. Kreisel
Department of Surgery, Washington University School of Medicine

Introduction: Neutrophilic graft infiltration is a hallmark of primary graft dysfunction (PGD) after lung transplantation. We have previously shown that monocytes promote extravasation of neutrophils into reperfused lung grafts after transplantation. The primary goal of this study was to investigate mechanisms how monocytes govern this process.

Methods: Wildtype (WT) B6 lungs ($CD45.1^+$)(18 h cold ischemia) were transplanted into $CD45.2^+$ B6 WT mice and evaluated at 24 hours unless stated otherwise. Using positron emission tomography (PET) imaging, flow cytometry and PCR we evaluated monocytic infiltration and neutrophil extravasation in grafts and expression of pro-inflammatory genes in monocytes. Some recipients were splenectomized before transplantation and received bone marrow derived-WT, IL1b- or MyD88-deficient monocytes. Tight junction proteins in IL1b-treated primary mouse lung endothelium were assessed by immunofluorescence. Lung endothelium permeability was assessed by measuring the fluorescence of FITC-labeled dextran across the endothelium monolayer. WT and MyD88-deficient monocytes were treated with mouse lung lysates and evaluated for IL1b expression.

Results: Splenectomizing recipients resulted in significant reductions in CCR2 signal by PET imagining and decreased numbers of $CD45.2^+Ly6c^+CD11b^+$ monocytes (1.1 vs 3.1 x 10^4 cells/mg; n= 6; $p<0.05$) in lung grafts. Compared to bone marrow monocytes, graft-infiltrating monocytes in control recipients expressed 4,500 times higher IL1b levels (2 hours reperfusion). The ratio of intravascular/interstitial neutrophils was significantly increased in lung grafts (1.6 ± 1.3 : 3.6 ± 1.3; n=6; $p<0.05$) and neutrophil numbers were reduced in airways (1.1 vs 2.4 x10^4 cells/ml; n=6; $p<0.05$) of splenectomized recipients. Injection of WT, but not IL1b- or MyD88-deficient splenic monocytes rescued neutrophilic extravasation in splenectomized recipients (intravascular/interstitial neutrophils WT : IL1b KO = 1.8 ± 1.5: 5.7 ± 3.9; WT : MyD88 KO = 1.2 ± 1.1 : 4.0 ± 1.6; n=4; $p<0.05$). Mouse lung lysates induced IL1b expression in mouse monocytes in MyD88-dependent fashion (n=4). IL1b treatment of primary mouse lung endothelium resulted in reductions in ZO-2 and Claudin-5 as well as tight junction disruptions (n=4), and an increase in endothelium permeability.

Conclusion: Our study has uncovered novel mechanisms that mediate PGD after lung transplantation. We identify the spleen as a reservoir for $CCR2^+$ monocytes that rapidly infiltrate reperfused lung grafts and promote extravasation of neutrophils through IL1b-mediated disruption of endothelial junctions. Monocytic IL1b production is at least in part activated through a MyD88-dependent pathway. Our findings provide a framework for the development of therapies for PGD by inhibiting neutrophil recruitment.

Characterization of peripheral nerve macrophages in health and disease

Peter Wang[1,2], Kiwook Kim[1], Jesse Williams[1], Jeffrey Milbrandt[2], and Gwendalyn Randolph[1]
[1]Division of Immunobiology and [2]Department of Genetics, Washington University in St. Louis

Introduction: Peripheral nerve and sensory ganglia macrophages are an underexplored population of cells involved in the feedback loop between environment and local immune response. Given their unique position on nerves that feed into specific organs, they represent a key population of cells for studying how intracellular interactions regulate physiological function in downstream targets. We find that these cells are present in several peripheral nerves, including the vagus nerve, which supplies fibers to the lung root and are involved in airway inflammatory diseases. The current project aims to explore PNS macrophage identity and function by examining their characteristics at steady state and under varied genetic and environmental conditions.

Methods: Confocal imaging was performed in CX3CR1 GFP/+ mice to visualize GFP-expressing cells in peripheral nerves, including dorsal root ganglia (DRGs), vagus, subcutaneous, and sciatic nerves. MPZ TdTomato reporter mice were used to visualize peripheral nerves. Flow cytometry confirmed GFP-expressing cells to be macrophages and was used to further identify macrophage and microglia-like subpopulations based on CD45 and GFP expression.

Results: Our preliminary data shows the existence of multiple populations of macrophages in peripheral nerves at steady state. We identify at least two subsets of PNS macrophages expressing microglia marker CX3CR1, including a radioresistant population with high CX3CR1 and low CD45 expression. These cells were found in fascia nerves that innervate subcutaneous adipose tissue, as well as in sensory ganglia, sciatic nerves, and vagus nerves. Currently, we are determining gene expression in these cells at steady state and under varied conditions.

Conclusion: By studying how local neuro-immune interactions affect tissue homeostasis in distal innervation targets, the proposed research attempts to understand how intrasystemic communication helps to coordinate complex cellular processes in various tissues. Importantly, this perspective may prove useful in airway inflammation research, as recent work has identified a connection between immune cells in the jugular nodose complex and allergic airway inflammation. Through our investigation of the vastly underexplored populations of PNS and ganglia macrophages, we expect to reveal basic principles in tissue biology that may extend into potential therapeutic strategies.

Epithelial cell signaling is a control point for follicular tuberculous granuloma formation

Oliver A. Prince[1], Javier Rangel-Moreno[2], Deepak Kaushal[3], Shabaana A. Khader[1]
[1]Department of Molecular Microbiology and Immunology, Washington University School of Medicine, St. Louis, Missouri. [2]University of Rochester Medical Center, School of Medicine and Dentistry, Rochester, New York. [3]Division of Bacteriology, Tulane National Primate Research Center, Covington, Louisiana; Department of Microbiology and Immunology, Tulane University School of Medicine, New Orleans, Louisiana

Introduction: *Mycobacterium tuberculosis* (*Mtb*) is the causative agent of pulmonary tuberculosis (TB), impacting one-third of the world's population. The tuberculous granuloma is a hallmark structure formed during the adaptive phase of TB. Formation of follicular granuloma is associated with control, however the host or Mtb factors that drive follicular granuloma remain elusive. We conducted a *Mtb* transposon screen in non-human primates in order to replicate natural human *Mtb* infection and observed that 44% of the mutants identified were cell wall mutants. We utilize the mouse model in order to elucidate the mechanism of follicular granuloma formation in the host induced by the Mtb mutants.

Methods: C57Bl/6, mice were aerosol infected with low dose (100 CFU) or medium dose (500 CFU) WT Mtb or ΔmmpL7. $Ikk2^{fl/fl}$ $Sftpc^{cre}$ mice are defective in NFkB signaling in type II airway epithelium and were paired with $Ikk2^{fl/fl}$ littermate controls prior to infection with low dose WT Mtb. Lungs were harvested at the acute stages of infection (day 15, 20, 40) and analyzed for lung cell accumulation (flow cytometry), cytokine expression (ELISA or Luminex) and pathology hematoxylin and eosin staining (H&E).

Results: We have identified a novel role for Mtb cell wall mutants that fail to induce granulocyte colony stimulating factor (G-CSF) in mouse epithelium in vitro and during aerosol infection of mice in vivo during acute infection. The defect correlates with decreased myeloid cell accumulation at 15 days post infection (dpi) and follicular granuloma at 40 dpi, absent during WT infection. In addition, low dose WT Mtb infection of $Ikk2^{fl/fl}$ $Sftpc^{cre}$ resulted in decreased in myeloid cell accumulation at 15 dpi and follicular granuloma formation at 40 dpi absent in $Ikk2^{fl/fl}$ littermate controls.

Conclusions: Epithelial levels of G-CSF, perhaps through NFkB, appears to fine tune tuberculosis granuloma formation during the acute phase by altering myeloid accumulation and subsequent TB granuloma distribution and follicular structure.

Common Immune Correlates of Tuberculosis Across Species

Thomas KA, Khader SA
Department of Molecular Microbiology, Washington University in St. Louis

Introduction: Over a third of the world's population is infected with *Mycobacterium tuberculosis* (*Mtb*), the causative agent of pulmonary tuberculosis (PTB). Multi-drug resistance of *Mtb* is on the rise, resulting in a larger global health burden. In order to produce better vaccines and/or treatments, it is of importance to define the immune mechanisms responsible for protection or for disease pathogenesis. By leveraging the immune features of disease severity and latency which are common across multiple experimental models of *Mtb* infection, one could identify those aspects most important to *Mtb* pathogenesis. Recent work by our collaborators identified a unique transcriptomic blood signature (16 genes) indicative of humans undergoing conversion to active disease (Zak 2016 *Lancet*). Of note, one of these genes, *Scarf1*, is a scavenger receptor important for clearance of apoptotic cells, and highly expressed by macrophages and dendritic cells. It has been demonstrated that apoptosis-mediated cross presentation of *Mtb* antigens is required for efficient adaptive immune responses to *Mtb* infection. We hypothesize that *Scarf1* contributes to mounting an effective adaptive immune response, and loss of function would result in increased susceptibility to tuberculosis.

Methods: We aerosol infected C57Bl/6 (B6) or *Scarf1*$^{-/-}$ mice with ~100CFU of a clinically relevant W-Beijing strain of *Mtb*, HN878, and assessed disease severity both during the acute (30 days post infection (*dpi*)) and chronic (60 *dpi*) stages of murine tuberculosis. Lungs and spleens of infected mice were homogenized, plated, and CFU measured to determine bacterial burden. Myeloid cell infiltrate was measured in single cell lung suspensions using flow cytometry. Cell death was assessed using Annexin V and 7-AAD staining in conjunction with flow cytometry.

Results: Absence of *Scarf1* did not significantly alter bacterial burden or cellular infiltrate at 30 *dpi*. During the chronic phase of infection, we found no differences in cellular recruitment, but did see significantly more lung cell necrosis in *Scarf1*$^{-/-}$ mice.

Conclusion: While not more susceptible to acute infection with the W-Beijing strain of *Mtb*, HN878, *Scarf1*$^{-/-}$ mice may have altered rates of cell death during chronic infection. While preliminary, these studies suggest that *Scarf1* may not play a significant role in *Mtb* pathogenesis in a mouse model of tuberculosis.

Host immune responses to multidrug resistant Mycobacterium tuberculosis

Nicole Howard[1], Bruce Rosa[2], Katya Loginicheva[3], Natalia Kurepina[4], Javier Rangel-Moreno[5], Fong-Fu Hsu[2], Maxim Artyomov[3], Robyn Klein[2], Makedonka Mitreva[2], Barun Mathema[4], Shabaana A. Khader[1]

[1]Department of Molecular Microbiology, [2]Department of Medicine, [3]Department of Pathology and Immunology, Washington University School of Medicine; [4]Department of Epidemology, Columbia University Mailman School of Public Health; [5]Division of Allergy/Immunology and Rheumatology, University of Rochester School of Medicine and Dentistry

Tuberculosis remains a public health crisis, and the emergence of drug resistant *Mycobacterium tuberculosis* (Mtb) strains has complicated treatment efforts. Unfortunately, little is known about the immune response to multi-drug resistant (MDR) Mtb. Therefore, we aimed to determine if the immune requirements of protection between drug sensitive and MDR Mtb strains were similar. To this end, we used a MDR Mtb clinical isolate, W7642, and compared it to a related drug susceptible isolate, HN878. We found that while there were some shared immune factors required for protection, *Il1r1*$^{-/-}$ mice were resistant to W7642 infection, suggesting that IL-1 signaling may be dispensable for that strain. Despite highly similar immune responses and pathology, RNAseq of the lung revealed many transcriptomic changes in *Il1r1*$^{-/-}$ mice when compared to C57Bl/6 wildtype mice infected with W7642, suggesting a large number of pathways were critical for maintaining resistance against MDR Mtb infection in the absence of IL-1 signaling. Additionally, we found a number of transcriptional changes between HN878 and W7642 infection in wildtype mice, suggesting that each strain provokes a unique response even when the immune compartment is intact. We hypothesized that because multidrug resistance is often associated with cell wall remodeling, it may influence the way in which MDR Mtb is sensed by the host immune system, leading to different immune requirements of protection. After screening other related MDR Mtb clinical isolates for their requirement for IL-1 signaling, we used whole genome sequencing to determine a short list of single nucleotide polymorphisms (SNPs) that could contribute to this phenomenon, including several SNPs associated with drug resistance or the cell wall. Together, the data suggest that MDR Mtb requires unique immune factors to maintain protection during infection.

Clinical Category

Single Nucleotide Polymorphism in a Gene Involved in Mycophenolic Acid Metabolism is Linked to Survival Post-Lung Transplantation

Laneshia Tague MD[1], Derek E. Byers MD, PhD[1], Ramsey Hachem MD[1], Andrew Gelman PhD[2]
[1]Department of Medicine, Division of Pulmonary and Critical Care, Washington University in St. Louis. [2]Department of Surgery, Division of Cardiothoracic Surgery, Washington University in St. Louis

Background: Immunosuppression in lung transplant recipients must strike a delicate balance between adequate rejection protection and drug toxicity and the maintenance of immunosurveillance. Prior studies have shown that single nucleotide polymorphisms (SNPs) in genes involved in mycophenolic acid (MPA) metabolism may lead to significantly different exposure to MPA. However, the effect on graft function and survival has not been reported in this population.

Methods: We conducted a single-center retrospective cohort study of adult lung transplant recipients from 2008 to 2013 receiving mycophenolic acid. Exclusion criteria included transplant before age 18, transplantation at another center and patients undergoing retransplantation. SNPs from the SLCO, UGT and ABBC2 families were chosen based on review of the literature on MPA metabolism. Genotyping was done by Taqman assay of saliva DNA. Our primary outcome was one year graft survival. Statistical analyses included student's t test and chi-square test for baseline demographic and clinical data, Kaplan-Meier curves with log rank test for equality of survivors and Cox regression modeling with inclusion of significant baseline variables.

Results: 218 patients met inclusion criteria, were able to provide an adequate DNA sample and were included in our study. SNP frequencies were comparable to expected population frequencies. SNP *rs4149117* in SLCO1B3 was associated with a significant difference in one-year graft survival (98.8% vs. 92.6% *p=0.015,* Figure 1). Cox regression modeling showed that risk of death at one year remained significantly higher for patients with the variant of *rs4149117* (HR 1.1-3.6, *p=0.04)*.

Conclusion: A SNP in the SLCO1B3 gene is associated with significantly decreased graft survival in lung transplant patients receiving mycophenolic acid. Further study is required to elucidate the underlying mechanism of this association and determine its clinical utility.

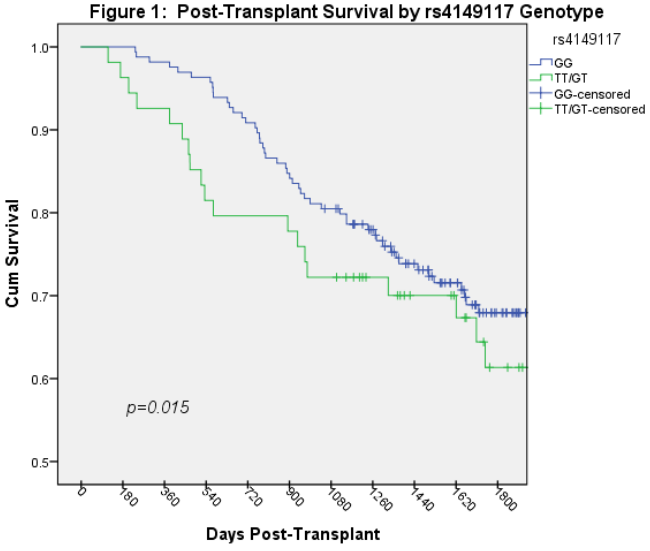

Airway Remodeling Measured by Targeted Biopsies in Severe Asthma

Chase Hall[1], Abhaya P. Trivedi[1], Charles Goss[1], Jonathan Boomer[1], Geneline Sajol[1], Jim Kozlowski[1], Ajay Sheshadri[2], Huiqing Yin Declue[1], David Gierada[1] Jered P. Sieren[3], Mark Escher[3], Melissa Saylor[3], Rebecca Schutz[1], Ken B. Schechtman[1], Sean Fain[4], Mark Schiebler[4], Nizar Jarjour[4], Ken Leader[5], John B. Trudeau[5], Sally Wenzel[5], Serpil C. Erzurum[6], Jason Lempel[6], Bruce Levy[7], Elliot Israel[7], George R. Washko[7], John V Fahy[8], Wendy C. Moore[9], Eugene R. Bleecker[9], Eric A. Hoffman[3], Mario Castro[1] on behalf of the NHLBI Severe Asthma Research Program (SARP)

[1] Washington University School of Medicine, St. Louis, MO, [2]The University of Texas MD Anderson Cancer Center, Houston, TX, [3]University of Iowa Carver College of Medicine, Iowa City, IA, [4]University of Wisconsin, Madison, WI, [5]University of Pittsburgh, Pittsburgh, PA, [6]Cleveland Clinic, Cleveland, OH, [7]Brigham and Women's Hospital, Boston, MA, [8]University of San Francisco, California, [9]Wake Forest University School of Medicine, Winston-Salem, NC

Rational: Airway remodeling in patients with asthma has been associated with progressive loss of lung function. A prospective study comparing multi-detector computed tomography (MDCT) airway measurements to airway histology is needed to validate a non-invasive technique for evaluating airway remodeling.

Methods: 145 well-characterized patients (55=severe asthma, 54=mild asthma, and 36=normal) from the Severe Asthma Research Program (SARP) underwent MDCT imaging of the chest using a standardized protocol. The MDCT was analyzed using quantitative software (Pulmonary Workstation, VIDA Diagnostics; Iowa City, IA) with wall area percentage (WA%) and wall thickness percentage (WT%) at each 3-4th generation. Each patient underwent bronchoscopy with endobronchial biopsies performed at two non-targeted sites and then two targeted sites (after un-blinding) using those segments with the highest WA%. All biopsy specimens were analyzed by two independent readers for epithelial (EPI) thickness and area, lamina reticularis (LR) area, basement membrane (BM) length, and total smooth muscle area. Biopsy generated remodeling parameters were correlated against CT generated parameters using a linear fixed effects and linear mixed model analysis.

Results: Baseline demographic data demonstrated patients were predominantly females (55%) and African American (55%). Patients in the severe asthma group had lower baseline lung function than the mild asthma group and normal controls (FEV_1 % predicted of 68%, 98% and 103%, respectively). There was a higher WT% and a trend towards higher WA% in the severe group compared to non-severe and normal controls (Table1). There was no difference in any of the biopsy-generated parameters of remodeling between the groups except for LR/BM length in the targeted biopsy group (9.91 ± 2.68 vs 9.48 ± 2.65, P=0.027). Overall, there were weakly higher correlations of targeted biopsies with CT measures compared with non-targeted biopsies but these did not achieve statistical significance.

Conclusions: Increased airway remodeling was noted in the severe asthma group compared to normal controls when assessed by quantitative MDCT. However, we did not demonstrate histologic evidence of remodeling across groups, which may be related to sampling error or the embedding technique utilized. MDCT may be a more sensitive technique for identifying airway remodeling in severe asthma.

Supported by the National Institutes of Health, National Heart, Lung, Blood Institute Severe Asthma Research Program.

Table 1:

Variable	Severe N= 55	Mild N= 54	Normal N= 36
Age at Enrollment	44.36 ± 11.38**	30.04 ± 10.85	30.74 ± 13.36
FEV1/FVC	0.67 ± 0.11**	0.77 ± 0.07	0.81 ± 0.08
FEV1% predicted	68.52 ± 21.15**	98.04 ± 24.87	103.31 ± 17.76
FVC % predicted	82.72 ± 21.54**	106.57 ± 26.31	108.21 ± 29.94
Maximum FEV1	2.60 ± 0.73**	3.89 ± 0.92	3.69 ± 0.97
Maximum FVC	3.68 ± 1.16**	4.68 ± 1.06	4.38 ± 1.09
WT%	19.09 ± 4.12**	17.67 ± 4.17	17.70 ± 2.93
WA%	63.95 ± 5.72*	60.51 ± 6.16	61.38 ± 5.40
LR/BM	9.72 ± 2.67*	10.08 ± 2.74	9.07 ± 2.5
Epi Area + LR Area /BM Length	35.20 ± 6.89	32.61 ± 7.63	34.35 ± 10.29
Smooth Muscle Area / Total Tissue Area	0.24 ± 0.11	0.21 ± 0.09	0.20 ± 0.07

Numeric data is expressed as mean ± SD, * = P-value ≤ 0.10, ** = P-value ≤ 0.05 across groups

Repeatability of CT Airway Measurements in Severe Asthma

Shweta Sood[1], Chase Hall[1], Abhaya P. Trivedi[1], Charles Goss[1], Jim Kozlowski[1], Ajay Sheshadri[2], David Gierada[1] Jered P. Sieren[3], Mark Escher[3], Melissa Saylor[3], Rebecca Schutz[1], Ken B. Schechtman[1], Sean Fain[4], Mark Schiebler[4], Nizar Jarjour[4], Ken Leader[5], John B. Trudeau[5], Sally Wenzel[5], Serpil C. Erzurum[6], Jason Lempel[6], Bruce Levy[7], Elliot Israel[7], George R. Washko[7], John V Fahy[8], Wendy C. Moore[9], Eugene R. Bleecker[9], Eric A. Hoffman[3], Mario Castro, MD[1] on behalf of the NHLBI Severe Asthma Research Program (SARP)

[1] Washington University School of Medicine, St. Louis, MO, [2]The University of Texas MD Anderson Cancer Center, Houston, TX, [3]University of Iowa Carver College of Medicine, Iowa City, IA, [4]University of Wisconsin, Madison, WI, [5]University of Pittsburgh, Pittsburgh, PA, [6]Cleveland Clinic, Cleveland, OH, [7]Brigham and Women's Hospital, Boston, MA, [8]University of San Francisco, California, San Francisco, CA, [9]Wake Forest University School of Medicine, Winston-Salem, NC

Background: Computer-aided analysis of airway dimensions on CT scans has demonstrated that automated image analysis software applied to the same images by different users results in highly repeatable measurements. The variation in measurements related to repeating the entire CT scan is unknown and may affect the ability to monitor patients for changes over time.
Methods: In the Severe Asthma Research Program (SARP) Ancillary Imaging Study, 57 subjects to date were characterized clinically (22 severe asthma, 25 non-severe asthma, 10 normal controls) and underwent two volumetric lung CT scans (supine, full inspiration). All subjects underwent two CT scans within a five to ten day period. Using Pulmonary Workstation software (VIDA Diagnostics), the cross-sectional wall area percent (WA%) and wall thickness percent (WT%) were measured at the segmental (generation 3) and more distal generations in 6 segments: 1, 4, and 10 of the right and left lungs. Repeatability was assessed by determining the difference between pairs of measurements with 95% confidence intervals (CI) and by intraclass correlation (ICC). Paired t-tests and ANOVA tests were used to compared WA% and WT% in patient populations.

Results: The WA% ICC was strong for the normal, mild and severe asthma groups (0.79, 0.74 and 0.93 respectively). ICC decreased in the more distal generations beyond generation 3. The WA% was nonsignificant between the two scans for all groups (P=0.36) across all generations indicating the software precisely measures this parameter between two scans. Similar results were seen in the ICC for WT% in normal mild and severe asthma cohorts (ICC = 0.81, 0.51, and 0.68 respectively). The highest reliability was in generation 3, 4, and 5 for control subjects and generation 3 and 4 for all asthmatics. The WT% was nonsignificant between the two scans (P=0.97). The ICC analysis for the controls, mild and severe asthmatics for WA% asthma cohorts demonstrated wide 95% confidence intervals. This was likely due to the small sample size. There was no statistically significant difference in either mean WT% or WA% in segments 1, 4, and 10 generations 3-6 of both the right and left lungs between the initial and repeat volumetric CT scans.

Conclusions: The repeatability of quantitative CT airway measurements on separate scans is substantial but may vary over different segments and generations. Such data may be useful to estimate the amount of change that can be reliably detected in longitudinal studies.

Supported by the National Institutes of Health, National Heart, Lung, Blood Institute Severe Asthma Research Program.

The Use of CT to Characterize Cluster Phenotypes in the Severe Asthma Research Program

Abhaya P. Trivedi, MD[1], Chase Hall, MD[1], Ajay Sheshadri, MD[2], Charles Goss, PhD[1], Jered P. Sieren, BS, RTR, MR, CT[3], Mark Escher, BA[3], Rebecca Schutz, RN[1], Huashi Li, MS[4], Ken B. Schechtman, PhD[1], Wendy C. Moore, MD[4], Eugene R. Bleecker, MD[4], Eric A. Hoffman, PhD[3], Sean Fain, PhD[5], Nizar Jarjour, MD[5], Mario Castro, MD[1]

[1] Washington University School of Medicine, St. Louis, MO, [2]The University of Texas MD Anderson Cancer Center, Houston, TX, [3]University of Iowa Carver College of Medicine, Iowa City, IA, [4]Wake Forest University School of Medicine, Winston-Salem, NC, [5]University of Wisconsin School of Medicine

Rationale: Unbiased analyses of patients in the Severe Asthma Research Program (SARP) have previously identified five distinct clinical phenotypes that differ in severity of illness and health care utilization. The clusters were derived from the original SARP 1 & 2 cross sectional cohort. Clusters 1 and 2 consisted of younger, female patients with early onset atopic asthma and normal lung function. Cluster 3 included older women with a higher BMI and late onset, non-atopic asthma. Patients in clusters 4 and 5 had a longer duration of disease and a severe reduction in lung function. SARP 3 is a longitudinal cohort of over 700 patients. A subset of SARP patients had multi detector row CT (MDCT) completed. We describe the MDCT characteristics of the previously defined clinical clusters in the SARP 1/2, & 3 cohorts.

Methods: 419 patients had baseline MDCT performed at total lung capacity (TLC) and functional residual capacity (FRC) that were available for analysis. Imaging was obtained within 2 hours of maximal bronchodilator testing. We analyzed MDCT with Apollo (VIDA Diagnostics, Iowa City). The following were measured at generation 3: wall thickness (WT), wall area (WA), wall thickness percent (WT%), wall area percent (WA%), and lumen area (LA). Lung density measurements of total volume, emphysema like lung or ELL (percent of lung density below -950 Hounsfield units at TLC), and air trapping or AT (percent of lung density below -856 Hounsfield units at FRC) were also measured. Analysis of variance was completed to evaluate mean differences among clusters. We also compared airway measurements between Clusters 1 & 2 (non severe asthma) and Clusters 4 & 5 (severe asthma). We adjusted for changes in the mean and variance due to study differences between the SARP 1/2 and 3 cohorts using a linear mixed model approach.

Results: The following measurements differed among the pre-specified clusters (ANOVA <0.05): LA, WA%, WT%, ELL, and AT. In pre-specified analyses comparing clusters 1 and 2 with clusters 4 and 5, clusters 1 and 2 had significantly lower WT%, WA%, and significantly larger LA and increased air trapping ($P < 0.0001$).

Conclusion: Patients with severe asthma have increased airway remodeling as measured by increased WT% and WA%. MDCT can enhance distinction between clinical cluster phenotypes. Further analysis is needed to determine if imaging characteristics can be used to identify patients that are at increased risk for future exacerbations and/or increased health care utilization.

Supported by the National Institutes of Health, National Heart, Lung, Blood Institute Severe Asthma Research Program.

CT Characteristics of Clinical Clusters

Variable	Cluster 1 N= 61	Cluster 2 N= 154	Cluster 3 N= 51	Cluster 4 N= 78	Cluster 5 N= 75	P-value
WT (mm)	1.5 ± 0.2	1.5 ± 0.2	1.5 ± 0.2	1.5 ± 0.2	1.5 ± 0.2	0.2659
WT %	17 ± 2.2	17.6 ± 2.3	17.2 ± 1.9	18.1 ± 2.4	18.3 ± 2.6	**<0.0001**
WA (mm^2)	29.6 ± 5.1	30.2 ± 5.8	30.7 ± 6	29.4 ± 5.8	28.6 ± 5.8	0.2075
WA %	60.2 ± 3	61.4 ± 3.2	61.8 ± 3.5	62.8 ± 3.6	64.2 ± 3.1	**<0.0001**
LA	20.4 ± 4.8	19.9 ± 5.3	20 ± 6.3	18.3 ± 5.3	16.9 ± 5.2	**<0.0001**
Total volume	5155.8 ± 1225.2	4988.6 ± 1395.3	4579.8 ± 1080.8	5002.1 ± 1387.3	5007.6 ± 1226.8	0.0979
ELL	56.9 ± 19.1	52.8 ± 20.5	47.1 ± 17.9	57.5 ± 17.9	54.6 ± 20.1	0.0206
AT	0.2 ± 0.3	0.5 ± 0.7	0.2 ± 0.1	0.8 ± 1.5	1.5 ± 1.7	**<0.0001**

Development of a Formal Intensive Care Unit Curriculum For Medicine Housestaff

Abhaya P. Trivedi, MD, Adam Anderson, MD
Washington University School of Medicine, St. Louis, MO, Division of Pulmonary & Critical Care Medicine

Rationale: The intensive care unit (ICU) offers extensive teaching opportunities given the broad range of clinical conditions evident in the patient population. Much of the teaching is performed at the bedside and significantly varies depending on the supervising physician. In addition, work hour restrictions may limit exposure to pathology and learning opportunities. In an effort to standardize teaching for all housestaff in the ICU, a formal curriculum was created and implemented.

Methods: We created 16 case-based lectures covering routinely encountered critical care topics. The lectures were piloted and certified by the ICU medical director. After approval, 4-week schedules were created for each rotation block, correlating with the housestaff rotation. An off-service pulmonary or critical care fellow provides the lecture Monday through Thursday at 7:30, with mandatory attendance for medical ICU housestaff. The on-service medical ICU fellow covers critical patient issues during the lectures. Feedback was solicited from the housestaff through a survey, and comments are taken into consideration as we expand and further develop the curriculum.

Results: A total of 37 residents and interns completed the feedback survey. A majority of the housestaff felt that the lectures improved their knowledge of managing critically ill patients. They also felt that the lectures should be continued during their residency training. Most of the housestaff agreed or strongly agreed that the format of the curriculum is compatible with their learning style. The housestaff did not feel as though the lectures were interfering with patient care. Some of the additional topics requested include (1) nutrition (2) imaging interpretation (3) advanced ventilator management.

Conclusion: We received positive feedback from the housestaff after the implementation of a dedicated ICU educational curriculum. Additional lectures will be added to the rotation based on their comments. Future steps include assessing the impact of the curriculum on housestaff knowledge in managing critically ill patients.

Assessment of a Critical Care Ultrasound Fellowship Curriculum

David T. Pham, Abhaya P. Trivedi, Adam L. Anderson
Washington University, School of Medicine, Division of Pulmonary and Critical Care

Rationale: Point of care (POC) ultrasound is a tool that is increasingly used in the intensive care unit in the diagnosis and management of critically ill patients. At most academic institutions such as our own, the majority of ultrasound education is informal teaching performed at the bedside. In an effort to standardize ultrasound training, we developed a formalized and structured curriculum that will occur over the course of an academic year. This program includes didactic sessions, interactive teaching, and monthly review of images. The goal of this educational initiative is to provide our critical care fellows a solid foundation to integrate POC ultrasound in their practice.

Methods: Before orientation, the first year fellows completed a pretest (P0), which assessed comfort level and incorporated 15 knowledge-based and video review questions. After the start of their fellowship, they completed a 4-hour hands-on teaching session, received 2 didactic teaching sessions, and attended 2 imaging review conferences. Three months after their pretest, they completed their first assessment of knowledge and comfort level (P1). They will complete another assessment at 6 (P2), 9 (P3), and 12 (P4) months. Each knowledge assessment is unique, but assesses the same core concepts and principles. We will compare the scores from the initial test to the subsequent tests to assess for improvement in knowledge and comfort with using POC ultrasound.

Results: From P0 to P1 there was no significant change in the average number of questions answered correctly, 8.71 to 7.86 (p-value 0.82). As a group, fellows reported to be more comfortable incorporating point of care ultrasound in clinical care. Comfort scores increased from P0 (3.29) to P1 (4.0) with a p-value <0.05.

Conclusion: Although the fellows have received various ultrasound educational sessions, their knowledge of POC ultrasound did not improve thus far in the academic year. One factor that could be contributing is that the fellows have had limited hands-on experience and practical application this early in their training. This also highlights the need for reassessment of this new curriculum to fit the educational needs of the fellows in training. We will continue to develop and expand the sessions, while assessing their knowledge throughout the academic year.

Prospective surveillance of all-cause pneumonia in mechanically ventilated patients.

Kristen Fisher, Tracy Trupka, Paul Juang, Scott Micek, Marin Kollef
Department of Medicine/Division of Pulmonary and Critical Care

Introduction: The current definitions for pneumonia classify patients based upon risk for pathogen resistance including the terms community-acquired pneumonia (CAP) for patients at less risk for resistance and hospital-acquired pneumonia (HAP), ventilator-associated pneumonia (VAP), and health-care associated pneumonia (HCAP) for patients who have risk factors for more resistant pathogens. However, these definitions have received much criticism. The ability to predict multi-drug resistance (MDR) has not been replicated consistently in clinical studies nor have these definitions been consistently predictive of outcomes. Viral pneumonia, which has become more easily identifiable, is also not included in the current definitions. The goal of this study is to identify a classification for pneumonia that is predictive of clinical outcomes among patients with respiratory failure in a medical intensive care unit (MICU) in a large academic hospital. We are reporting preliminary data on the first 262 patients enrolled in a prospective study that classifies pneumonia based upon pathogen type.

Methods: We are conducting a prospective observational study of all mechanically ventilated patients with pneumonia admitted to the MICU at Barnes-Jewish Hospital from January 11, 2016 to January 10, 2017. Included patients meet a clinical diagnosis of pneumonia defined by a radiographic infiltrate in addition to two of the following criteria: 1) WBC >10,000 or <4,000 x 10^9/L; (2) temperature >38.6 ^{0}C or <36^{0}C; (3) purulent secretions from the lower respiratory tract; (4) PaO2/FiO2 ratio less than 300. Baseline characteristics including demographics, prior hospitalization or use of antibiotics, co-morbid conditions, immunosuppressive status, and severity of illness based upon APACHE II scores are collected. The patients are classified based upon pathogen type into the following categories: 1) antibiotic sensitive, 2) antibiotic resistant, 3) pathogen negative, and, 4) viral pneumonia. Antibiotic resistance is defined as resistance to ceftriaxone. Clinical outcomes are analyzed based upon these classifications using univariate statistics.

Results: This analysis included the first 262 patients in the study in which 44 (16.8%) patients are classified as antibiotic susceptible, 66 (25.2%) as antibiotic resistant, 90 (34.4%) as pathogen negative, and 62 (23.7%) as viral pneumonia. Preliminary results are summarized in Table 1 comparing baseline characteristics, severity of illness, and clinical outcomes classified by pathogen type.

Conclusion: Based upon these preliminary results, there are statistically significant differences in clinical outcomes when classifying pneumonia based upon pathogen type in mechanically ventilated patients. Given advances in rapid microbiologic diagnostics, this type of classification scheme may have advantages for assessing patient outcomes.

Table 1. Clinical outcomes for mechanically ventilated patients with pneumonia classified by pathogen type (n=262 patients).

	Antibiotic Susceptible n=44	**Antibiotic Resistant n=66**	**Pathogen Negative n=90**	**Viral n=62**	**P-value**
Age	58.8 ±15.9	59.6 ± 14.9	59.1 ± 15.9	57.0 ± 14.5	0.831
Charlson Score	3[2,6]	3 [1.3,4]	3 [1,4.3]	3 [2,4]	0.483
APACHE II	22[18.3,27]	25 [20,32]	24 [19,28.5]	23 [19,27]	0.162
Mortality*	31.8%	48.5%	31.1%	37.4%	0.132
Hospital LOS	15 [7,21.5]	17 [8,30.3]	11 [6, 20]	19.5[11,33.3]	**0.003**
ICU LOS	8 [4, 15.8]	9 [6,15]	7 [3,12]	8 [4,19.3]	0.125
Ventilator Days	4[2.3,10.3]	7 [3, 12]	4 [2,8]	6 [2.8, 13]	0.074
Antibiotic Days	9 [6, 14]	12 [6, 14]	7 [5,9]	7 [4,12]	**0.001**
Vasopressor Days	2[2,4]	4[2,8]	3[1,4]	5[2,11.5]	**0.019**

*Mortality comparing antibiotic resistant to pathogen negative pneumonia was statistically significant, p=0.04. LOS = length of stay.

Antibiotic De-escalation for Patients with Respiratory Failure

T. Trupka, MD, K. Fisher, MD, M. Kollef, MD, P. Juang, PharmD, S. Micek, PharmD
Washington University, Department of Pulmonary/Critical Care, St. Louis College of Pharmacy

Introduction: Empiric antibiotic choice is strongly linked to outcomes in sepsis. Increased utilization of broad-spectrum antibiotics has led to increasing numbers of multi-drug resistant (MDR) pathogens associated with increased mortality. By implementing antibiotic stewardship and/or de-escalation protocols, broad-spectrum antibiotic usage can be reduced and the previously up trending rates of MDR pathogens stabilized and in some cases even reduced. The aim of our study is to prospectively evaluate the effects of implementing an antibiotic de-escalation protocol based on acquired, real-time bacterial culture and viral PCR data rather than traditionally defined CAP, HAP, H-CAP, and VAP.

Methods: From January through December of 2016, patients admitted to the two medical intensive care units (MICUs) at Barnes-Jewish Hospital were screened for respiratory failure requiring invasive mechanical ventilation and concurrent administration of empiric antibiotics for lower respiratory tract infection (LRTI). Each MICU had a dedicated antibiotic stewardship team manually reviewing patient charts for clinical and infectious data daily for 6 months of the total study period. Patients were classified as having a non-infectious source of respiratory failure or infected with either a viral, antibiotic-sensitive (Ceftriaxone sensitive), antibiotic-resistant (Ceftriaxone resistant), or pathogen negative LRTI. For patients showing clinical improvement within 48-72 hours of antibiotic initiation and culture collection, recommendations for antibiotic de-escalation were provided via a simplified algorithm based upon these unique qualitative classifications. The 6 months in which each MICU was without a dedicated stewardship team served as the control data. Intent-to-treat analysis of baseline characteristics, antibiotic days, antibiotic de-escalation, ICU LOS, hospital LOS, and mortality were performed using chi-square, independent T-tests, ANOVA, and univariate analyses.

Results: (to date) 274 patients were screened, 73 were excluded, 201 were enrolled in the study, 97 (48%) in the enhanced stewardship arm and 104 (52%) in the control arm. Baseline characteristics between the two groups including comorbid conditions, pre-existing immunosuppression, and severity of illness (APACHE II) were similar. There was no significant difference between the rates of failure of initial antibiotic regimen (defined as refractory disease, death, or antibiotic-escalation), antibiotic de-escalation, total antibiotic days, or mortality between the groups.

Conclusion: In a high-acuity intensive care unit that has placed an emphasis on antibiotic stewardship for over 10 years, further implementation of a culture based de-escalation protocol does not significantly decrease antibiotic administration either by reducing duration of treatment or spectrum of coverage. Thus, the maximum impact of such an intervention is extremely limited and further focused efforts to improve antibiotic stewardship may be better serviced outside of the intensive care unit setting.

	Enhanced Stewardship (97)	Standard of Care (104)	p-value
Antibiotics De-escalated	44 (45%)	48 (46%)	0.910
Failure of De-escalation	3 (7%)	6 (13%)	0.359
Total Antibiotics Days for LRTI	6.0 [4.0, 8.5]	7.0 [3.3, 9.0]	0.983
Failure of Initial Antibiotics	29 (30%)	28 (27%)	0.640
Mortality	37 (38%)	28 (27%)	0.089

RISKS FOR COPD IN HIV-INFECTED INDIVIDUALS USING SYMPTOM-BASED SCORES AND SPIROMERTRY

Hlatshwayo, M, Sahagun, A, Presti, R, Atkinson, J
Department of Medicine, Division of Pulmonary and Critical Care

Background: Pulmonary complications are a significant source of morbidity in HIV-infected persons. Due to improved HIV infection treatment and high levels of smoking, chronic non-infectious respiratory co-morbidities have become prevalent among HIV-infected patients. Obstructive lung disease occurs in 7-9% of HIV+ persons, but a third of patients report respiratory symptoms. This project aims to define the relationship between symptom-based scores and pulmonary function tests, chest imaging, tobacco exposure and HIV disease severity.

Methods: HIV-positive and HIV-negative participants over age 30 who are current smokers with at least a 15 pack-year smoking history were enrolled. Pulmonary function tests were performed to assess for obstructive defect. St. George's Respiratory questionnaires (SGRQ) were administered and served as the primary source for symptom-based data. CT scans were performed to evaluate for underlying lung disease. All patients underwent basic demographic data collection as well as HIV disease specific information, including CD4 count and HIV viral load.

Results: This study included 75 HIV-infected patients and 38 HIV-negative controls. HIV-infected patients had lower tobacco exposure than HIV-negative patients (27.1 versus 46.4 pack-years), were younger (49.1 ± 8.0 vs 56.1 ± 7.0), and had less obstruction as demonstrated by higher FEV1/FVC ratio. Despite this, symptom-based scores were similar (26.9±20.7 vs 28±25.4, $p>0.05$), suggesting symptomatology may be a result of complex interactions between smoking, HIV, and COPD. Within the HIV-infected population, SGRQ scores were found to be most associated with pack year smoking history. Decreased FEV1/FVC ratio was associated with age, suggesting that the prevalence of clinical obstruction is likely to increase as overall survival improves.

Conclusion: This study underlines the importance of long-term study in the smoking, HIV-infected population in order obtain a better understanding of the role of HIV, tobacco, and aging in respiratory symptoms and the development of chronic respiratory co-morbidities.

Parameter	HIV +	HIV –	p-value
	Demographic Characteristics		
N	75	38	
Age, year	49.1 ± 8.0	56.1 ± 7.0	<0.001
Male, (%)	57 (77.3%)	24 (63.2%)	
African American (%)	60 (80%)	29 (76.3%)	
BMI	27.1 ± 6.0	28.8 ± 5.0	0.119
	Respiratory Status		
Smoking	75 (100%)	38 (100%)	
Pack Year	27.3 ± 17.9	46.4 ± 14.4	<0.001
FEV1 % Pred	95.9 ± 15.0	88.3 ± 25.0	0.102
DLCO % Pred	58.3 ± 12.3	56. ±14.4	0.548
FEV1/FVC	0.79 ± 7.5	0.72 ± 13.6	0.008
<0.70 FEV1/FVC	9 (12%)	12 (31.6%)	
	SGRQ		
Total	27.1 ± 19.9	28.5 ± 25.4	0.770

Risk factors for the development of donor-specific HLA antibodies and their impact on outcomes after lung transplantation

K. Tsui[1], D.E. Byers[1], R.D. Yusen[1], A. Gelman[2], L. Tague[1], Y. Furuya[1], R.R. Hachem[1].
[1] Pulmonary/Critical Care Medicine, Washington University, St. Louis, MO, [2] Cardiothoracic Surgery, Washington University, St. Louis, MO

Purpose: Lung transplantation is an effective treatment for end-stage lung disease, but long-term outcomes remain disappointing. Median survival after transplantation is only 5 years and the leading cause of death is chronic lung allograft dysfunction (CLAD). Two phenotypes of CLAD have been recognized: bronchiolitis obliterans syndrome (BOS) and restrictive allograft syndrome (RAS). Donor-specific HLA antibodies (DSA) are associated with an increased risk of developing CLAD and worse survival, and a role for DSA in the development of RAS has been suggested. We hypothesize that lung injury promotes inflammatory pathways necessary for the development of DSA, which subsequently leads to CLAD. We also hypothesize that asymptomatic DSA is consistent with subclinical antibody mediated rejection (AMR) that progresses to RAS. The primary purpose of this study is to identify risk factors associated with the development of DSA, with an interest in causes of lung injury such as primary graft dysfunction (PGD), acute cellular rejection (ACR), and respiratory infections as well as the impact of DSA on outcomes such as CLAD and AMR.

Methods: We will enroll all patients transplanted between July 1, 2005 to December 31, 2015 at Barnes-Jewish Hospital and follow up will be complete through December 31, 2016 to allow a minimum of 1 year of follow-up. Exclusion criteria will be HLA desensitization prior to transplant and positive HLA crossmatch at time of transplant. The primary endpoint will be the development of DSA. Secondary endpoints will be development of CLAD (BOS or RAS), AMR, allograft survival, patient survival, and the impact of antibody depleting therapies on clinical outcomes. Statistical analysis will be performed in SPSS with plans to derive a statistical model using a derivation cohort, and validate the model with a validation cohort.

Histoplasmosis in adult lung transplant recipients

Yuka Furuya M.D., Chad Witt M.D., Elbert P. Trulock M.D., Derek Byers M.D. Ph.D., Roger Yusen M.D., Ramsey Hachem M.D.
Division of Pulmonary and Critical Care Medicine, Department of Internal Medicine

Introduction: This retrospective study was conducted to characterize the clinical presentation, treatment, and clinical course of *H. capsulatum* infection in lung transplant recipients at a large Midwestern academic medical center.

Methods: Cases of histoplasmosis in lung transplant recipients at our institution diagnosed between 2010-16 were identified. Disseminated histoplasmosis was defined as clinical, laboratory or imaging evidence of involvement of 2 or more organs.

Results: Six cases of Histoplasma infection were identified. The age at diagnosis ranged from 22 to 67 years. (Median 39.5). The pre-transplant diagnoses included IPF (1), CF (3) and COPD (2), and duration from transplant to diagnosis ranged from 4.6 to 219.9 months (Median 87). All cases were diagnosed by urine Histoplasma antigen (Ag). Fungal cultures grew *H. capsulatum* from blood in two cases, and from BAL in one case. Four cases had disseminated histoplasmosis. Fever was the most common presenting symptom (4/6). Other symptoms included respiratory failure (2/6), decline in FEV1 or FVC (2/6), GI symptoms and weight loss. One case presented with paresthesia and was found to have positive CSF Ag, and on MRI, brain lesions compatible with CNS Histoplasmosis *(Figure 1)*. Another presented with pericardial effusion. All cases were initially treated with IV liposomal Amphotericin. Acute kidney injury limited duration of Amphotericin in three patients. In all patients, treatment with an azole was continued for ≥ 3 months, and patient had a clinical response and a decrease in Ag load. Therapy was completed in two patients after an average of 11.6 months after urinary Ag cleared, and in two patients, azole was continued lifelong. In the remaining two patients, treatment is ongoing. Two patients died of chronic lung allograft dysfunction (CLAD) and mortalities were not attributed to Histoplasma infection.

Conclusion: Histoplasma infection in lung transplant recipients is most commonly manifested by fever. All cases were treated with IV Amphotericin followed by an azole, and resulted in clinical response. There were no fatalities from Histoplasma infection.

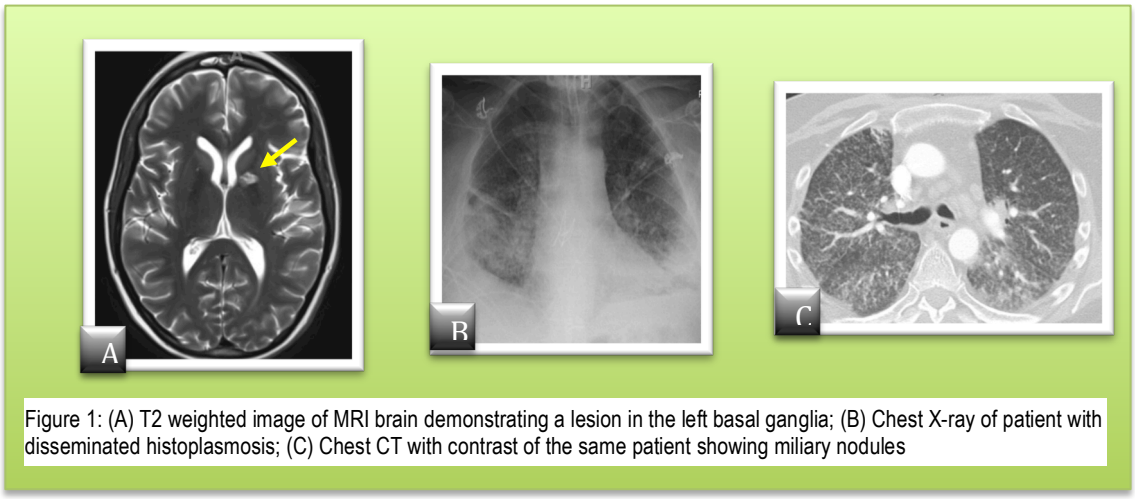

Figure 1: (A) T2 weighted image of MRI brain demonstrating a lesion in the left basal ganglia; (B) Chest X-ray of patient with disseminated histoplasmosis; (C) Chest CT with contrast of the same patient showing miliary nodules